

# On Enhancing HTGR Lower Plenum Heat Transfer and Mixing via Swirling Jets

**Sal B. Rodriguez<sup>1,2</sup> and Mohamed S. El-Genk<sup>2</sup>**

<sup>1</sup>*Sandia National Laboratories, P.O. Box 5800, MS 0748, Albuquerque, NM 87185-0748,  
sbrodri@sandia.gov, (505) 284-2808*

<sup>2</sup>*Chemical and Nuclear Engineering Dept. and Institute for Space and Nuclear Power Studies,  
Albuquerque, NM 87131, mgenk@unm.edu, (505) 277-5442*

**Abstract** - Operating high temperature gas-cooled reactors (HTGRs) at elevated temperatures brings about unique challenges in the lower plenum (LP), such as hot spots and thermal stratification. Analysis performed using Sandia National Laboratories' (SNL) Fuego computational fluid dynamics (CFD) code shows that these issues can be mitigated using static swirling inserts at the exit of the helium coolant channels in the LP. A full-scale, half-symmetry LP section of a prismatic-core HTGR is modeled using a numerical mesh that consists of 5.5 million hexahedral elements. The LP model includes the graphite support posts, the helium flow channel jets, the bottom plate, and the exterior walls. Calculations are performed for both conventional jets and clockwise and counter-clockwise swirling jets, varying the swirl number,  $S$ , from 0 to 2.49. Our calculations show that increasing  $S$  increases mixing in the LP by enhancing heat transfer and mixing, thus reducing the likelihood of forming hot spots and thermal stratification.

## I. INTRODUCTION

There is current interest in the development of Next Generation Nuclear Plants (NGNPs) and high temperature gas-cooled reactors (HTGRs). Key designs include the pebble bed and prismatic cores.<sup>1</sup> However, the high operation temperature of these helium cooled reactors (873 - 1,223 K) presents structural, operational, and safety challenges.<sup>1</sup> Of particular concern in the prismatic core HTGR are the “hot spots” in the bottom plate and thermal stratification of the helium coolant in the lower plenum (LP). The hot spots are caused by the impingement of the hot helium jets exiting the reactor core at  $> 60$  m/s onto the bottom plate. The stratification, however, is caused by the poor mixing of the helium coolant in the LP, aggravated by the obstruction of the graphite support columns (Fig. 1). The motivation for this work is to reduce the

likelihood of formation of hot spots and helium stratification. This is achieved by stimulating more mixing in the LP and the impingement of the hot helium exiting the coolant channels in the reactor core. These results are realized through reducing the axial momentum, while increasing the angular momentum of the exiting helium jets.<sup>2-8</sup> The acquired azimuthal velocity increases entrainment of the surrounding helium, causing the velocity field to spread radially with distance and to entrain more of the adjacent, cooler gas. These processes inevitably enhance the mixing and heat transfer within the LP.

The acquired azimuthal momentum also weakens the impingement of the hot helium onto the bottom plate in the HTGR LP, thus reducing the likelihood of hot spots. These improvements in performance and operation safety of HTGRs are possible by altering the nature of the hot helium flow exiting the coolant channels in the HTGR

core from conventional to swirling jets; more on that later.

Recent theoretical studies and experiments have been reported which investigate free conventional and swirling jets for mass and heat transfer applications.<sup>2-13</sup> However, investigations of the flow fields of single and multiple swirling hot gas jets at the temperatures of interest in HTGRs are limited.<sup>5-8</sup> Unlike liquids, the dynamic viscosity of gases increases with temperature, while stabilizing the flow field. Viscosity also affects the flow mixing and the entrainment of surrounding gas into the flow field of a swirling jet.

Furthermore, the flow field involving multiple swirling jets, such as an HTGR LP, becomes very complex. Of particular interest to HTGR operation and safety is to quantify the effects of cross-flow and solid obstructions due to the graphite support columns on the characteristics and the mixing of the jet flow (Figs. 1 and 2). Investigations of the latter are almost nil as of 2010.<sup>7,14</sup>

Key flow phenomena expected to occur in the LP of a prismatic core HTGR (Fig. 2) include multiple jet flow field interaction and mixing, cross flow entrainment and mixing, flow around the cylindrical graphite support columns, vortex shedding, cross-flow, impinging, and the Coanda effect.<sup>14</sup> Additionally, there would be regions of high Reynolds number (Re), flow transition and recirculation, vortex interaction and instability, and mixing enhancement/suppression as well as stagnation zones. The Fuego CFD code<sup>15</sup> is employed to investigate these complex and multidimensional flow fields. This comprehensive code is currently being developed at Sandia National Laboratories (SNL). It is the objective of the ongoing research at the University of New Mexico and SNL to continue to address such a complex issue in relation to the operation and safety of HTGRs and NGNPs.

The objective of the work presented herein is to investigate the potential of using swirling jets at the exit of the coolant channels in a prismatic core HTGR to minimize or eliminate the

formation of hot spots in the bottom plate and to enhance flow mixing in the LP. We also investigate the effect of changing the swirl number (S) and the rotation direction of the swirling jets. The following section briefly describes the Fuego CFD code used in the present analysis.<sup>15</sup>

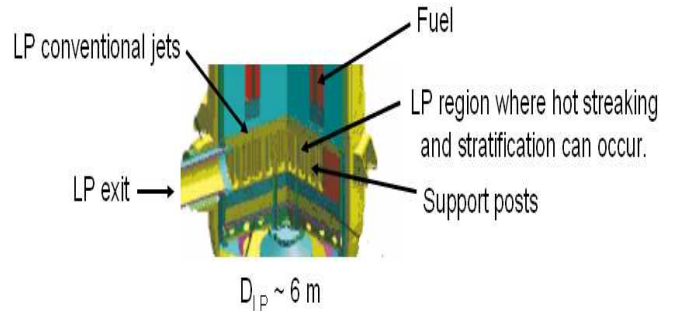


Fig. 1. A cut-away view in the LP in a prismatic core HTGR.<sup>1,14</sup>

## II. FUEGO CFD CODE

Fuego is a 3D, incompressible, reactive flow, massively parallel, generalized unstructured CFD code with state-of-the-art turbulence models, which contain the RANS and large eddy simulation (LES) models. The RANS models include v2-f, low Re k- $\epsilon$ , standard k- $\epsilon$ , as well as many others. Among Fuego's more sophisticated LES models are the KSGS, Smagorinsky, and dynamic Smagorinsky.

Whenever there is complex, 3D turbulence and mixing, as is the case in the HTGR LP, the v2-f, Smagorinsky, and dynamic Smagorinsky models are ideal. The commercial CFD code FLUENT has been used by Idaho National Laboratories to model the flow turbulence and mixing in the LP using conventional jets.<sup>14</sup>

Fuego has recently undergone key validation and verification (V&V) studies that include: (1) conventional jets (axial and radial velocity distribution, jet spreading angle), (2) swirling jets (axial and azimuthal velocity), (3) conventional jet in cross-flow (jet propagation, jet velocity, production of counter-rotating vortices, jet cross-section), and (4) flow around a vertical cylinder

(pressure distribution, formation of vortex, vortex shedding).<sup>7</sup>

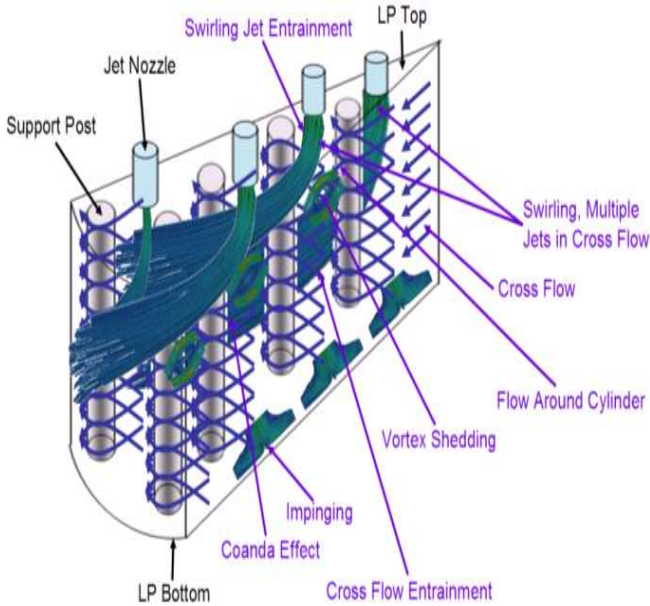


Fig. 2. Key flow regimes in the LP of a prismatic core HTGR.

### III. LP INPUT MODEL

The HTGR LP Fuego input model (Fig. 3) used in the present simulations invoked the dynamic Smagorinsky LES turbulence model, and was run on the massively parallel Thunderbird machine at SNL. The initial time step used is 0.1  $\mu$ s, and the simulation transient time varied from 100 ms to several seconds.

The computation mesh used in the present calculations consists of 1 to 5.5 million hexahedral elements. It is generated using the CUBIT code<sup>19</sup> from geometry developed with Pro/ENGINEER.<sup>20</sup>

Note that the geometry, and the thermal and flow BCs (boundary conditions) used for this research are partially arbitrary, as no final, official VHTR design has been published in the literature. However, the values used herein are consistent with those found in the literature. Additionally, the literature contains a wide myriad of geometric, thermal, and flow parameters. Nevertheless, the values used in this research are “ball park”, and yield results that

can be easily extrapolated to those of the final design, should there ever be one.

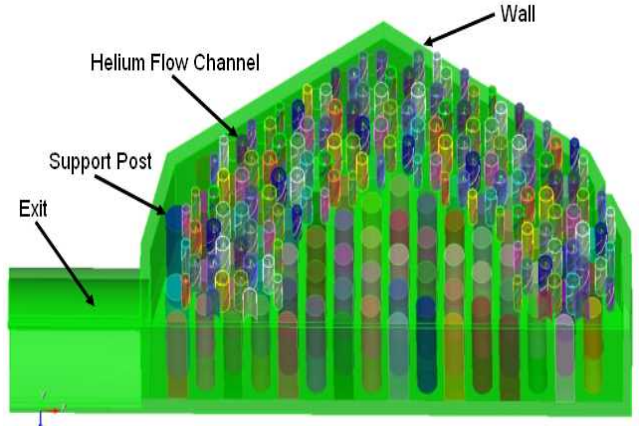


Fig. 3. Half-symmetry of the simulation model of the LP in an HTGR.

In these simulations, the velocity of the hot helium gas exiting the coolant channels in the HTGR core for a conventional jet was chosen as  $V_o=60$  m/s in the  $+z$  direction, which is also the approach velocity to the swirl insert at the exit of the coolant channels. The emerging gas flow from the coolant channels acquires three dimensional principal velocity components,  $u$ ,  $v$ , and  $w$ , depending of the swirl angle of the insert,  $\theta$ . As noted in our previous research,<sup>8</sup> the swirling field can be generated numerically in various forms, such as helicoidal swirl geometry that is subsequently meshed, or by employing a set of swirl BCs. Because it is easier to employ the BCs, we will follow this approach for our current research.

The swirl angle for a hubless swirl device is related to  $S$  as:<sup>16-18</sup>

$$S = \frac{2}{3} \tan(\theta) \quad (1)$$

The velocity components can be approximated as 3D helicoids:<sup>8</sup>

$$\mathbf{V}_o(x,y,z) = u_o \sin(2\pi y) \mathbf{i} - u_o \sin(2\pi x) \mathbf{j} + w_o \mathbf{k}, \quad (2)$$

where

$$\frac{u_o}{V_o} = \frac{v_o}{V_o} = \frac{1}{\left[2\left(1 + \frac{4}{9S^2}\right)\right]^{\frac{1}{2}}}, \quad (3)$$

and

$$\frac{w_o}{V_o} = \frac{2}{3S} \frac{1}{\left(1 + \frac{4}{9S^2}\right)^{\frac{1}{2}}}. \quad (4)$$

The interested reader is referred to Ref. 8 for a derivation of Eqs. 3 and 4, as well as for the reasoning for choosing Eq. 2 as our helicoid velocity field.

#### IV. SIMULATION RESULTS AND DISCUSSION

A set of calculations is performed to investigate the impact of swirl rotation direction of the hot helium exiting the LP coolant channels. A second set of calculations is performed to investigate the impact of changing S on the mixing and heat transfer in the LP. The results of these calculations are presented and discussed in the subsections that follow.

##### IV.A. Conventional Jets vs. Clockwise and Counter-Clockwise Swirling Jets

Three calculations are performed to compare the effect of S and the swirling jet rotation direction: conventional jets (base-case), clockwise (CW) swirling jets, and counter-clockwise (CCW) swirling jets. The base-case calculation has 138 conventional helium jets (S=0). The second calculation involves the same number of swirling jets, but has S=0.67 and all jets rotate in the CW direction. The third calculation is the same as the second, except that all the jets swirl in the CCW direction.

For the base-case calculation, the principal velocity components for 135 jets are:

$$(u, v, w)_{\text{conv}} = (0.0, 0.0, 60.0) \quad (5)$$

This velocity distribution follows the helicoidal velocity field distribution found in Eq. 2. However, because the conventional jet field does not rotate, the sinusoidal terms are set to 0. The velocities are in m/s and the helium gas temperature emerging from the coolant channels is 1,273 K (or 1,000 °C). The three remaining jets are at the same velocities, but with higher helium gas temperature set to 1,473 K. These hotter jets are distributed across the LP as shown in Fig. 4. They represent “hot channels” and also serve as tracers for the flow field in the LP.

For the CW swirling jets calculation, the velocity components for 135 jets are given as:

$$(u, v, w)_{\text{CW}} = [-21.2\sin(2\pi y), 21.2\sin(2\pi x), 51.96] \quad (6)$$

The velocity distribution again follows the helicoidal velocity field distribution found in Eq. 2. The velocities are in m/s and the helium gas temperature is 1,273 K, while the remaining three jets are at the same velocities, but at a higher helium temperature of 1,473 K. The hotter jets are in the same location in the LP as in the base-case calculation (Fig. 4).

For the CCW swirling jet calculation, the velocity components for 135 jets are given as:

$$(u, v, w)_{\text{CCW}} = [21.2\sin(2\pi y), -21.2\sin(2\pi x), 51.96] \quad (7)$$

Once again, this velocity distribution follows the helicoidal velocity field distribution. The velocities are in m/s and the helium gas temperature is 1,273 K, while the remaining three jets are at the same velocities, but at a higher helium temperature of 1,473 K. The hotter jets are in the same location in the LP as in the base-case calculation (Fig. 4).

Thus, except for the jet boundary conditions, the three calculations use the same input deck, mass flow rate per BC, mesh, code version, and number of parallel processors.

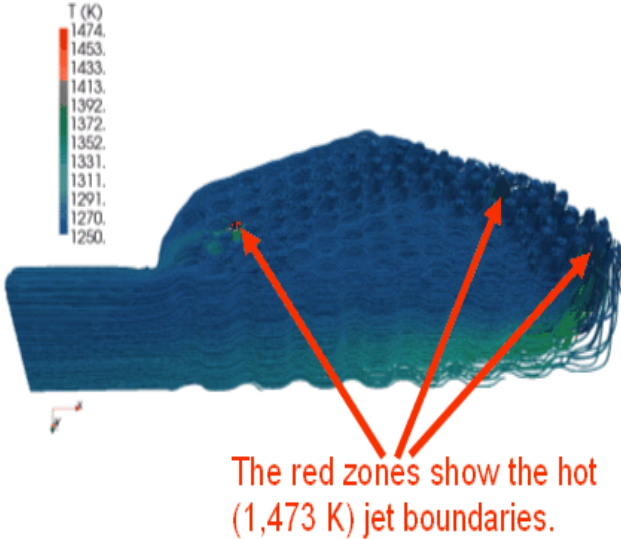


Fig. 4. Location of hot channels in the LP model.

To simplify the comparison process, Fig. 5 shows the results for a single jet in the base-case (conventional jet) vs. a single CCW swirling jet (the entire flow field for all 138 jets is found in Fig. 4). As Fig. 5 shows, the advantages of the CCW swirling jets over the conventional jets are: (1) the CCW swirling jet diameter is  $\sim 70\%$  wider and therefore distributes its thermal energy over a wider volume within the LP, (2) the upper portion of the swirling jet's flow field shows  $\sim 50\%$  more entrainment of the surrounding helium in the LP, and (3) at half the jet height, the swirling jet is  $\sim 50$  K cooler. Because the swirling jets entrain more of the surrounding gas that subsequently mixes with the hotter gas of the jet, the thermal stratification observed with conventional jets is minimized.

A comparison of the calculated flow fields in the LP with CW and CCW jets is shown in Fig. 6. As expected, the helicoid's CCW motion in the  $+z$  direction effectively opposes the general flow direction in the LP (towards the LP exit as the gas flows to the energy conversion assembly); see Fig. 7. This opposing flow increases turbulence and mixing, and therefore enhances heat transfer. As shown in Fig. 6, the CW swirling motion results in less enhancements in turbulence, mixing, and heat transfer than the

CCW swirling motion. Nevertheless, its impact is higher than conventional jets (base-case), as a comparison of Figs. 5 and 6 shows.

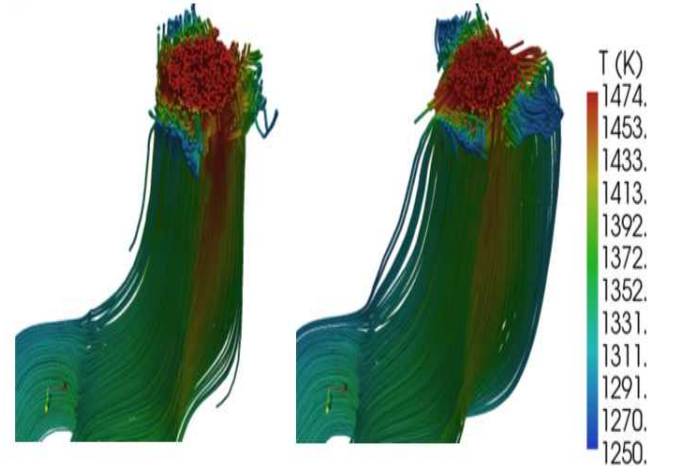


Fig. 5. Comparison of the calculated jet flow fields: view of a single jet. LHS: base-case (conventional jet). RHS: CCW swirling jet.

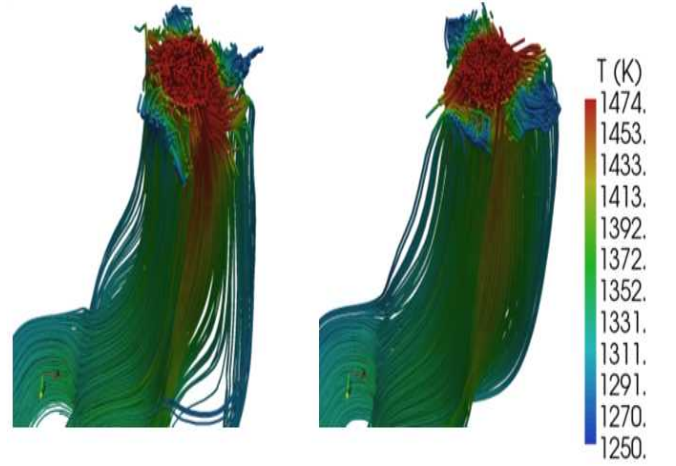


Fig. 6. Comparison of the calculated swirling jet flow fields: view of a single jet. LHS: CW jet. RHS: CCW jet.

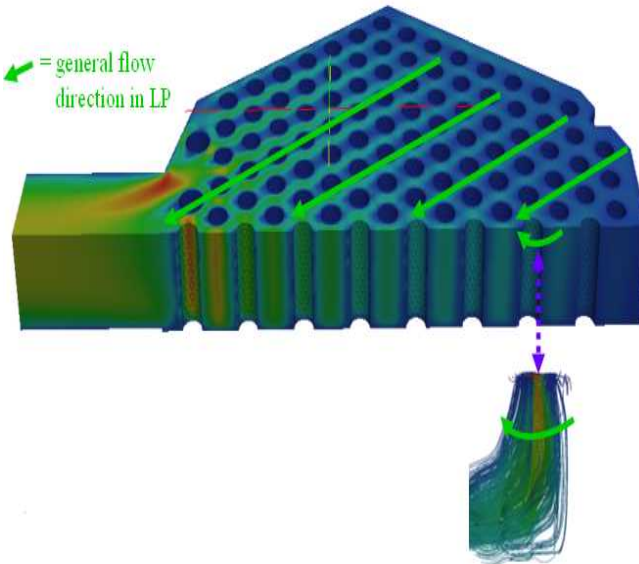


Fig. 7. Importance of rotation direction for the swirling jets.

#### IV.B. Effect of $S$

Flow field calculations in the HTGR LP are performed to investigate the effect of  $S$  on mixing, and enhancements in turbulence and heat transfer. Calculations are performed for  $S=0$  (i.e.,  $\theta=0^\circ$ , conventional jet), and for swirling jets for which  $S=0.38, 0.67, 1.15$ , and  $2.49$  (i.e.,  $\theta=30, 45, 60$ , and  $75^\circ$ , respectively). The five calculation sets are with the same helium temperatures as the base-case (i.e., three channels are hotter than the other 135 channels).

To quantify the effect of  $S$  on cooling the bottom plate in the HTGR LP, the hexahedral element cell-averaged temperatures of a planar slice at the bottom plate (the opposite end of the jet exits) are calculated and grouped according to a linear temperature distribution ("bins"). The calculated temperature bins are shown in Fig. 8. The figure shows that as  $S$  increases, the number of finite elements in the bottom plate with cooler temperature increases (see arrow on LHS of Fig. 8). In addition, there are fewer hotter finite elements (as shown by the arrow pointing downward, on the RHS of Fig. 8). Furthermore, as  $S$  increases, the entrainment of the surrounding helium increases linearly, in agreement with the literature.<sup>16</sup> Consequently, by

the time  $S=2.49$ , all the finite elements in the temperature slice are only within  $1 - 2$  K of the surrounding, cooler helium jets.

Figure 9 presents the cooling effect on the bottom plate when using conventional jets (top) and swirling jets (bottom). Note that for  $S=0$ , the flow field of the hottest helium conventional jets eventually reaches the bottom plate at slightly lower temperature of  $\sim 1,325$  K. However, with the swirling jets at  $S=2.49$ , the gas thoroughly mixes, decreasing the temperature of the helium reaching the bottom plate by an additional 52 K, that is, to  $\sim 1,273$  K. Furthermore the temporal distribution in the bottom plate is not only lower but also more uniform, as shown by the arrows in Fig. 9.

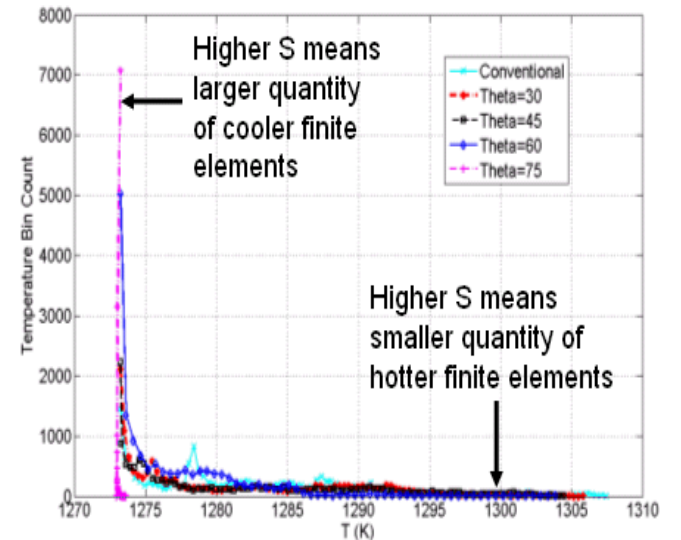


Fig. 8. Effect of  $S$  on heat transfer enhancement at the bottom plate in the HTGR LP.

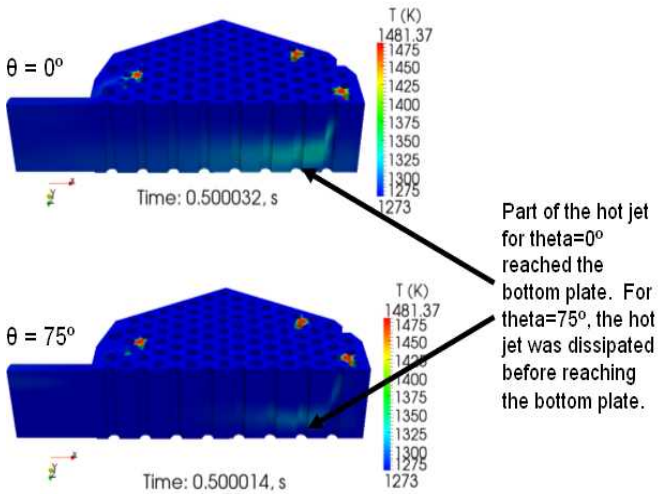


Fig. 9. Comparison of results for conventional vs. swirling jets. Top: Conventional ( $\theta=0^\circ$ ,  $S=0$ ). Bottom: Swirling ( $\theta=75^\circ$ ,  $S=2.49$ ).

## V. SUMMARY AND CONCLUSIONS

Analysis is performed using SNL's Fuego CFD code to investigate swirling jet inserts at the exit of the helium coolant channels of an LP for a prismatic core HTGR. The goal was to reduce the likelihood of forming hot spots in the bottom plate, and to eliminate thermal stratification by enhancing heat transfer and mixing.

A full-scale, half-symmetry LP section of the prismatic-core HTGR is modeled using a numerical mesh that consists of 5.5 million hexahedral elements. The developed LP model accounts for the graphite support posts, the helium flow channel jets, the bottom plate and the exterior walls. Calculations are performed for conventional jets, as well as CW and CCW swirling jets. Additionally,  $S$  is varied from 0 to 2.49. Results show that swirling jets enhance heat transfer and flow mixing, thus reducing the temperature of the bottom plate in the LP, as well as enhancing its temperature uniformity. Swirling jets also increase entrainment of surrounding helium and mixing in the LP, which increases as  $S$  increases.

The results with CCW swirling jets ( $S > 0$ ) show more enhanced mixing and entrainment than with CW swirling jets, which in turn results

in more mixing and entrainment than conventional jets ( $S=0$ ). The flow field diameter of the CCW swirling jets is up to 70% wider than conventional jets, and thus able to distribute the thermal energy over a wider volume. Secondly, the upper portion of the CCW swirling jet experiences  $\sim 50\%$  more entrainment than conventional jets. Therefore, at half the jet height, the swirling jets are  $\sim 50$  K cooler than conventional jets.

With  $S \geq 2.49$  (or  $\theta \geq 75^\circ$ ), the bottom plate is cooler, its temperature is more uniform, and there is more mixing of the helium in the LP. With conventional jets, the helium flow field reaches the bottom plate at  $\sim 1,325$  K, whereas with swirling jets at  $S=2.49$ , the helium flow reaches the bottom plate at  $\sim 1,273$  K. Furthermore, the helium more thoroughly mixes in the LP with higher  $S$ .

## ACKNOWLEDGMENTS

The authors thank Stefan Domino at SNL for his help with Fuego.

## NOMENCLATURE

BC	Boundary condition
CCW	Counter-clockwise
CFD	Computational fluid dynamics
CW	Clockwise
D	Diameter of coolant jets (m)
G	Gas mass flux, $\rho V$ (kg/m <sup>2</sup> s)
HTGR	High temperature gas-cooled reactor
LES	Large eddy simulation
LP	Lower plenum
NGNP	New Generation Nuclear Plant
Re	Reynolds number, $GD/\mu$
S	Swirl number
u	Velocity in x direction (m/s)
v	Velocity vector consisting of (u, v, w) components (m/s)
w	Velocity in y direction (m/s)
VHTR	Very high temperature reactor
V&V	Validation and verification
w	Velocity in z direction (m/s)

x	Cartesian x coordinate
y	Cartesian y coordinate
z	Cartesian z coordinate (direction of jet flow for S=0)
$u_0$	Azimuthal velocity (m/s)
$\theta$	Swirl angle ( $^{\circ}$ )
$\mu$	Dynamic viscosity (Pa·s)
$\rho$	Gas density (kg/m <sup>3</sup> )
	Subscripts
conv	Conventional jet ( $\theta=0^{\circ}$ , S=0)
o	Constant parameter for S=0 at jet outlet

## REFERENCES

1. G. A. JOHNSON, "Power Conversion System Evaluation for the Next Generation Nuclear Plant (NGNP)", Proc. International Congress on Advances in Nuclear Power Plants (ICAPP '08), American Nuclear Society, Paper # 8253, Anaheim, CA (2008).
2. L. HUANG and M. S. El-Genk, "Heat Transfer of an Impinging Air Jet on a Flat Surface", *Int. J. Heat and Mass Transfer*, **Vol. 37**, No. 13, 1915 – 1923 (1994).
3. L. HUANG and M. S. El-Genk, "Heat Transfer and Flow Visualization Experiments of Swirling, Multi-Channel, and Conventional Impinging Jets", *Int. J. Heat Mass Transfer*, **Vol. 41**, No. 3, 583 – 600 (1998).
4. M. S. EL-GENK and L. Huang, "An Experimental Investigation of the Effect of the Diameter of Impinging Air Jets on the Local and Average Heat Transfer". *J. Heat and Technology*, **Vol. 17**, No. 1, 3 – 12 (1999).
5. RODRIGUEZ, S. B. and M. S. El-Genk, "Using Helicoids to Eliminate 'Hot Streaking' and Stratification in the Very High Temperature Reactor Lower Plenum", *Proceedings of ICAPP '08*, American Nuclear Society, Paper 8079, Anaheim, CA (2008).
6. RODRIGUEZ, S. B. and M. S. El-Genk, "On Eliminating 'Hot Streaking' and Stratification in the VHTR Lower Plenum Using Helicoid Inserts", *HTR-08*, American Society of Mechanical Engineers, Paper 58292, Washington, DC (2008).
7. RODRIGUEZ, S. B. and M. S. El-Genk, "Numerical investigation of potential elimination of 'hot streaking' and stratification in the VHTR lower plenum using helicoid inserts", *Nuclear Engineering and Design Journal* (2010). In press as of January 2010.
8. RODRIGUEZ, S. B. and M. S. El-Genk, "Heat Transfer and Flow Field Characterization of a Triangular Array of Swirling Jets Impinging on an Adiabatic Plate", *14<sup>th</sup> International Heat Transfer Conference*, Washington DC, (2010). (Draft submitted for review).
9. T. CZIESLA *et al.*, "Large-Eddy Simulation of Flow and Heat Transfer in an Impinging Slot Jet", *Int. J. Heat and Fluid Flow*, **Vol. 22**, No. 5, 500-508 (2001).
10. B. MERCI and E. Dick, "Heat Transfer Predictions with a Cubic k- $\epsilon$  Model for Axisymmetric Turbulent Jets Impinging onto a Flat Bed", *Int. J. Heat Mass Transfer*, **Vol. 46**, No. 3, 469-480 (2003).
11. J. LAROCQUE, "Heat Transfer Simulation in Swirling Impinging Jet", Institut National Polytechnique de Grenoble, Division of Heat Transfer (2004).
12. P. WANG and X.S. Bai, "Large Eddy Simulation and Experimental Studies of a

Confined Turbulent Swirling Flow”, *Physics of Fluids*, **Vol. 16**, No. 9, 3306-3324 (2004).

13. A. KING, “Heat Transfer Enhancement and Fluid Flow Characteristics Associated with Jet Impingement Cooling”, Ph.D. Diss., Curtin University of Technology, Australia (*circa* 2005).
14. D. M. MCELIGOT and G. E. McCreery, “Scaling Studies and Conceptual Experiment Designs for NGNP CFD Assessment”, Idaho National Laboratory, INEEL/EXT-04-02502 (2004).
15. SNL, SIERRA/Fuego/SYRINX Low Mach Fluids/Radiation Transport Code, Sandia National Laboratories, <https://engsci.sandia.gov/1500, FactsheetDocs/Fuego.pdf> (2006).
16. N. M. KERR and D. Fraser, “Swirl. Part I: Effect on Axisymmetrical Turbulent Jets”. *J. of the Institute of Fuel*, **Vol. 39**, 519 – 526 (1965).
17. M. L. MATHUR and N. R. L. MacCallum, “Swirling Air Jets Issuing from Vane Swirlers. Part 1: Free Jets”, *Journal of the Institute of Fuel*, **Vol. 40**, 214-225 (1967).
18. K. BILEN, K. Bakirci, S. Yapici, and T. Yavuz, “Heat Transfer from a Plate Impinging Swirl Jet”, *Int. J. Energy Res.*, **Vol. 26**, 305-320 (2002).
19. CUBIT,  
<http://www.cs.sandia.gov/capabilities/CubitMesherProgram/index.html> (2009).
20. PRO/ENGINEER,  
<http://www.ptc.com/products/proengineer> (2009).